Aerodynamic Coefficients Investigation of GRAD Rocket using Computational Fluid Dynamics

Ammar Eltaj and Sakhr Abudarag

Aeronautical Engineering Department, Sudan University of Science and Technology, Khartoum, Sudan
sakhr.abudarag@sustech.edu

Received:15/01/2021
Accepted:28/10/2021

ABSTRACT- The article provides an aerodynamic characteristics investigation of GRAD Rocket using the computational fluid dynamic method. Computational analysis has been performed to predict the Aerodynamic characteristics of the GRAD rocket. A commercial software ANSYS FLUENT is used to simulate the unsteady aerodynamic characteristics of the missile while the Missile DATCOM software is used to confirm and validate the results. The simulations have been conducted out for a range of Mach number 0.4 to 3 versus angle of attack from 0° to 9°, through the sideslip angle 0° to 9°. The results represent that the Drag Coefficient is highly sensitive to the angle of attack and velocity region. The total drag of the missile is mainly generated from the missile's body, where they wrap around fins contribute only 18.45 percent of a total drag coefficient. In contrast, the lift coefficient increases with an increased angle of attack, but it decreases with changes of the region from subsonic to supersonic. The flow visualization of the static and dynamic pressure contours is illustrated. The Shock wave is captured at the nose and fins entrance. To verify the results, the simulations were carried out for two missile models. The first model represents the cylindrical body of the fin-less missiles, and the second one represents the rocket body with fins.

Keywords*: Aerodynamic properties; Full propellant Missile; Wrapped around fins; CFD; DATCOM.*

المستخلص – تستعرض الورقة دراسة الخصائص الإيروديناميكية لصاروخ GRAD باستخدام طريقة ديناميكية الموائع التحسيبية. تم إجراء التحليل الحوسبي بإستخدام برنامج ANSYS FLUENT لمحاكاة الخصائص الإيروديناميكية للصاروخ بينما تم استخدام برنامج Missile DATCOM لتأكيد النتائج والتحقق منها. تمت المحاكاة عند سرعات تتراوح من 0.4 إلى 3 ماخ مقابل زاوية هجوم من 0 درجة إلى 9 درجات وزاوية إنزلاق جانبي من 0 درجة إلى 9 درجات. أشارت النتائج إلى أن معامل المقاومة يتأثر بشدة بزاوية الهجوم والسرعة. أكدت النتائج أن المقاومة الكلية للصاروخ تتولد بشكل أساسي من جسم الصاروخ بينما تساهم الزعانف بنسبة 18.45% فقط. بالمقابل يزداد معامل الرفع مع زيادة زاوية الهجوم لكن يتناقص مع تغير السرعة من دون سرعة الصوت إلى فوق سرعة الصوت. تم أيضاً عرض خطوط كنتور الضغط الساكن والديناميكي حول الصاروخ لتحديد موضع موجة الصدمة عند رأس الصاروخ ومدخل الزعانف.

Introduction

Due to the high cost of experimental investigation mainly the wind tunnel experiment in developing Rockets performance, the simulation programs have become very important as a preliminary design tool in various engineering applications. Moreover, the determination of aerodynamic forces and moment coefficients using classical methods is difficult and it is not precise enough, especially for complicated geometries and high-speed regions. Developed CFD techniques are considered as a robust method that has been used to determine and validate the aerodynamic quantities of flying objects, and ANSYS, FLUENT software is one of these tools with fully capable to simulate and determine many applications. In this article, ANSYS, FLUENT software has been used to simulate and determine the aerodynamic coefficients for GRAD-developed rockets. The 122 mm Grad Rocket is propelled by a self-contained rocket motor. At present, it is considered as a weapon system that is mostly equipped and widely used all over the world. The structure consists of a conical nose shape and four wrapped around fins to reach a 20 km maximum range [1]. It is a priority to use the numerical techniques for the determination

of aerodynamic coefficients which are considered as input data for other applications such as the design of guidance and control systems, preparing firing tables, and trajectory calculations.

Literature review

The development of the supersonic GRAD rocket has been covered by extensive research during the last twenty years. For example, Slobodan et al [2] obtained the rolling moment coefficients for two models with a wrap-around wing and one model with a flat wing. They proved that the rolling moment coefficient at zero angle of attack is equal to the sum of the rolling moment coefficient due to the curvature of the fins and the rolling moment coefficient of the canted equivalent flat fins. Also, they represented that the rolling moment coefficient is a function of the angle of attack.

Ravi Krishna et al [3] represented the results of a numerical study to understand the flow field over a projectile with wrap-around fins. Their investigation was performed to determine aerodynamic coefficients for the missile model for varying Mach numbers from 1.2 to 2.5.

Their results showed a reversal of the rolling moment in a Mach number from 1.2 to 1.4. While generating Mach number profile along missile body, a transition from subsonic to supersonic flow was notably found just before the fin-tip in the Mach number range from 1.2 to 1.4.

This transition from subsonic to supersonic just before the fin seems to be the main cause for the rolling reversal, which makes the flow inside the fin passage behave differently. Also, Attapon, et al [4] introduced a new way to find the aerodynamic characteristic equation of missiles for the numerical trajectory prediction more accurately. They used commercial CFD software to solve flow simulation with tetrahedron elements and the boundary conditions are specified by two variables velocity and angle of attack.

The equations are formed by curve fitting, data obtained from simulation. The equations were constructed in form of perpendicular force, axial force, and moment which depended on two variable parameters, velocity, and angle of attack, and the obtained equation has power 3 of velocity term as we expected and corresponded with the classical aerodynamic theory.

Moreover, F. Mingireanu et al [5] conducted a full 6 DOF modeling for a GRAD rocket in Earth's non-inertial frame. They presented a 6 DOF modeling with various step-like thrust curves while maintaining the same total impulse delivered by the original motor.

The influence of the step size of the range of the GRAD rocket is investigated together with the dispersion influence. They showed that a significant range increase can be obtained while using the same propulsion unit with a step-like thrust-curve modification. Also, they investigate the influence of the step-like thrust curve on the dispersion of such a rocket and the technological possibilities to implement their solution.

In addition, Chun-Chi Lia, et al [6] studied integrated a low-speed wind tunnel experiment, CFD, and MATLAB/Simulink to analyze the aerodynamic attributes and simulate flight trajectories of a tail fin-stabilized projectile with two shapes. The Karman-Tsien rule was used to revise and convert the air compressibility of the low-speed wind tunnel trials data into subsonic wind tunnel 0.6 Mach data, which could subsequently reduce costs.

The results of two types of projectiles showed that the aerodynamic coefficients CD, CL, CM, and CMα of the converted experiment data were similar to the computational data within an angle of attack within +/-8°. Besides this, Guo Qing, Zhang et al [7] investigated the aerodynamic characteristics, to analyze the impacts generated by different parameters of wraparound fins (WAFs) and to find the corresponding mechanism.

They showed that the WAF configurations can greatly improve the longitudinal stability and enhance the longitudinal aerodynamic characteristics for the whole rocket.

The total drag of the whole rocket mainly stems from the body, the extra side forces and rolling moments are due largely to the unequal pressure distributions on both sides of the fin (windward or leeward). Maintaining a certain negative setting angle, δ, can effectively avoid the coning movement and improve the flight stability at high angles of attack.

Modeling & Simulation

The geometry and the mesh of the missile and domain were generated with GAMBIT software as shown in Figures 1 and 2.

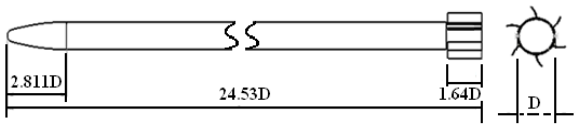

Figure 1: Geometry configuration and dimensions

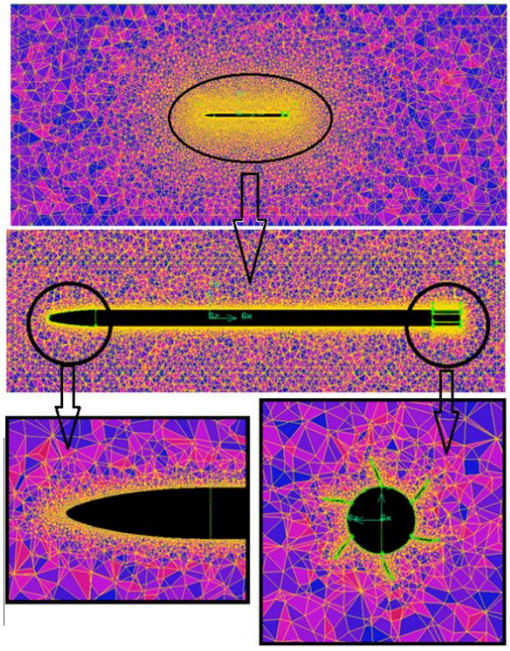

Figure 2: Computational Mesh

Computational Mesh

The method of single domain technology is used and the size function option is used to generate a mesh of the flow domain The number of mesh elements was 1,547073 elements and the boundary condition were set up according to Table 1.

TABLE.1: BOUNDARY CONDITIONS SET UP

Boundary	Description	Type
Back-face	The close surface at the end of the missile	Mass flow rate
Far	The domain of flight	Pressure far field
Wing	Fins of missile	Wall
Body	missile body	Wall

Mathematical model & Governing Equations

The governing equations of compressible Newtonian fluid flow are [8]:

Continuity Equation:

$$\frac{\partial \rho}{\partial t} + \nabla \cdot (\rho \boldsymbol{V}) = 0 \qquad (1)$$

Momentum Equation:

$$\rho \left[\frac{\partial \boldsymbol{V}}{\partial t} + (V \cdot \nabla)\boldsymbol{V}\right] = -\nabla p + \mu \nabla^2 \boldsymbol{V} \qquad (2)$$

Energy Equation:

$$\frac{\partial (\rho i)}{\partial t} + \nabla \cdot (\rho i \boldsymbol{V}) = p\nabla \cdot \boldsymbol{V} + \nabla \cdot (k \nabla T) + \emptyset + S_i \qquad (3)$$

where, $i = C_v T$

Turbulence Model

The SST k-ω model is designed to avoid the freestream sensitivity of the standard k-ω model, by combining elements of the ω-equation and the ε-equation [8]. In addition, the SST model is calibrated to accurately compute flow separation from smooth surfaces within the k-ω model family. Therefore, the SST model is used to capture the turbulence predicting in the research. The SST model is one of the most widely used models for aerodynamic flows. It is typically more accurate in predicting the details of the wall boundary layer characteristics than the Spalart-Allmaras model.

The transport equations of the SST k-ω model are:

Kinetic Energy Equation:

$$\frac{\partial (\rho k)}{\partial t} + \frac{\partial (\rho k u_i)}{\partial x_i} = \frac{\partial}{\partial x_j}\left(\Gamma_k \frac{\partial k}{\partial x_j}\right) + G_k - Y_k + S_k \qquad (4)$$

where, $\Gamma_k = \mu + \frac{\mu_t}{\sigma_k}$, $G_k = \mu_i S^2$, $S \equiv \sqrt{2 S_{ij} S_{ij}}$, $Y_k = 2\rho\omega M_i^2$, and $M_i \equiv \sqrt{\frac{k}{\gamma RT}}$

Specific Dissipation Rate:

$$\frac{\partial (\rho \omega)}{\partial t} + \frac{\partial (\rho \omega u_i)}{\partial x_i} = \frac{\partial}{\partial x_j}\left(\Gamma_\omega \frac{\partial \omega}{\partial x_j}\right) + G_\omega - Y_\omega + D_\omega + S_k \qquad (5)$$

where, $\Gamma_\omega = \mu + \frac{\mu_t}{\sigma_\omega}$, and $\mu_t = \propto \frac{\rho k}{\omega}$

Solution Strategy

A density-based solver with an implicit formulation was used and the velocity formulation was chosen to be absolute and Least Square Cell-Based gradient option was used. The fluid used for the flow field was taken as air with properties of ideal gases, operating condition was set as standard sea-level conditions for the simulation work.

The discretization of the momentum equation, energy equation, and conservation equation was done using a second-order up-winding scheme. Aerodynamic forces and moments were monitored

at each iteration to figure out the solution convergence and solution stability.

Turbulence computational fluid dynamics simulations were performed in SMT's high-performance computing system (Super Computer) and parallel CPUs were used for this study. The simulations were done with a maximum current number of 5 for all Mach numbers.

In case of high angle of attack and high speed the simulation was started with a low current number value of 1 and ramped up to the maximum value during the iterations of the simulation and the solution was converged more than 9,000 iterations depending on the Mach number, angle of attack and geometry. The convergence was determined by tracking the change in the flow, residual, and the aerodynamic coefficient plots have confirmed the stability during the solution.

Results and Discussions

To verify that the results obtained by the CFD method are correct the simulations were carried out for two missile models. The first model represents the cylindrical body of the finless missile, and the second one represents the rocket body with fins.

This classification is considered because this type of missile has wrap wings, and it is difficult to define the wrap fins in the Missile DATCOM program. The program deals only with planar fins of standard shapes, which is considered one of the limitations of this technique.

The Missile DATCOM program understands the wrap fins as flat fins when it is called from its library and then starts the calculation of the aerodynamic coefficients. Therefore, a slight difference in results is observed between the analytical and computational solutions. The technique used to verify and confirm the results of the CFD method with the MD program is considered the cylindrical body of the missile without fins as the first model and run both software for subsonic and supersonic regions with Mach numbers 0.8 and 4.0 respectively. The results reveal satisfactory agreement between the two solutions in both the high subsonic region and supersonic flow region as shown in Figures 3 and 4.

Figure 3.a. shows the total drag force coefficient for the missile's body in the high subsonic region (M=0.8). The two solutions have the same tendency, but there is a slight difference ranging approximately from 2 to 9 ° angle of attack between the Computational Fluid Dynamics method and the Missile DATCOM method.

This difference results from the fact that the Missile DATCOM software calculates the aerodynamic coefficients based on the dimensions of the body that inputted to the software. These dimensions are affected by the boundary layer, so the CFD considered the boundary layer effect which means the diameter of the missile increased to be equal original diameter plus the thickness of the boundary layer which in turn have a strong impact on the base drag and thus affects the total value of the drag coefficient.

Figure 3. b represents the total drag force coefficient for the missile's body in the supersonic region (M=4). The two methods have the same tendency and the figure shows a satisfactory agreement between the CFD method and the Missile DATCOM method. In the supersonic region, the effect of the boundary layer is very small because flow detaches the body due to shock wave appearance and then the wave drag is dominated.

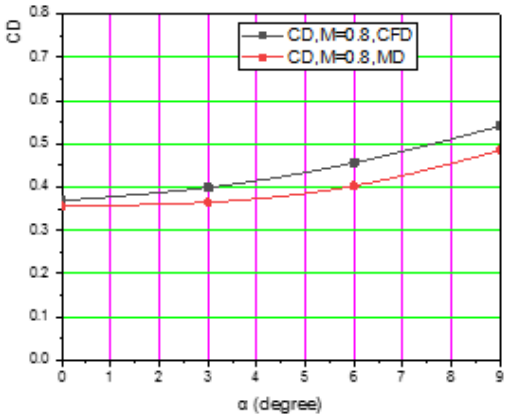

Figure 3. a: Total Drag force in the subsonic region

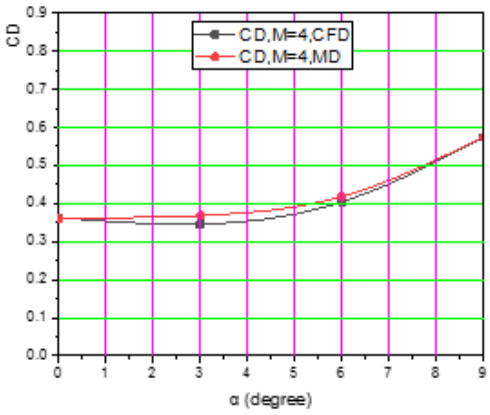

Figure 3. b: Total Drag force in the supersonic region

Figure 4. shows the lift force coefficient for the missile's body in the subsonic region The same behavior is captured by the two software and there is a slight difference between the Computational Fluid Dynamic method and Missile DATCOM method. The figure reveals that the lift coefficient increases with the increase of angle of attack.

Figure 4. b indicates the lift force coefficient for the missile's body in the supersonic region. The figure reveals a very satisfactory agreement between the computational and analytical results.

The previous results show an excellent agreement between the two techniques that have been used for the supersonic region while slight divergence is observed for the subsonic regime therefore, the Missile DATCOM software can be considered as a results validation tool indicating the accuracy of the computational fluid dynamics, CFD, approach.

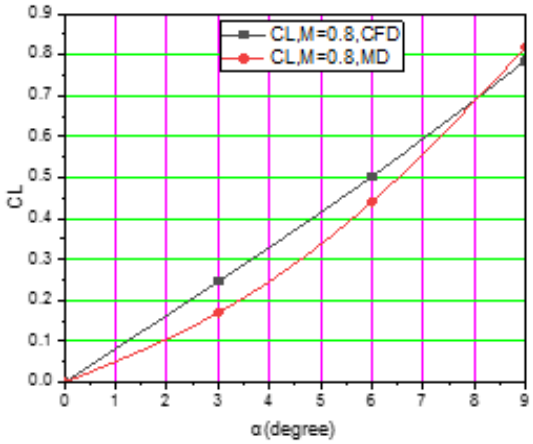

Figure 4. a: Lift force in the subsonic region

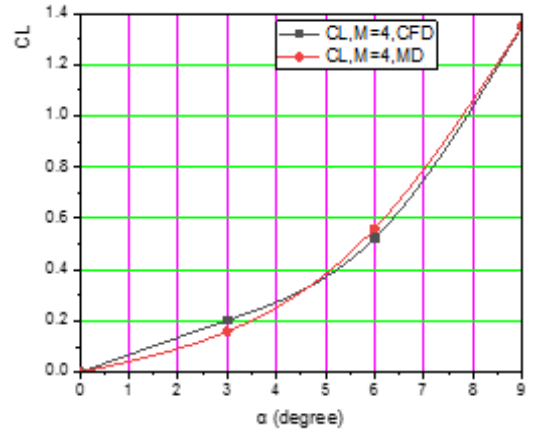

Figure 4. b: Lift force in the supersonic region

Full Configuration Model

The main task is to predict the aerodynamic characteristics of the missile geometry represented by the full configuration model which includes the missile body with wrap fins.

Drag Force Coefficient

Figure 5 (a and b) shows the total drag force coefficient for the missile at various regions of speed against the range of angle of attack. Figure 5.a. indicates the total drag force coefficient for the missile in the subsonic regime (M=0.4) versus a range of angles of attack. From the Figure, the two solutions provide the same tendency of the drag coefficient and there is a slight difference in CD between the CFD method and Missile DATCOM method starts to increase regularly after the angle of attack 3 degrees. At an angle of attack of 9 degrees, the Drag coefficient reaches 0.17.

Figure 5.b. illustrates the total drag force coefficient for the missile in supersonic flow regime at Mach number 2 against a range of angle of attack. The increment in drag coefficient occurs with an increase in the angle of attack. The drag coefficient at zero angles of attack is 0.3670 and 0.3295 read by the Missile DATCOM method and the CFD method respectively, whereas the coefficient at 9 ° is 0.5540 and 0.53142 indicated by Missile DATCOM technique and the CFD technique respectively.

As shown in Figure 5 (a and b) the value of drag coefficient computed by CFD has a little delay from that computed by Missile DATCOM, this delay is referred to as three reasons. Firstly, the missile DATCOM uses free stream velocity at the missile's nose and fins entrance, but CFD uses corrected velocity due to the flow deceleration.

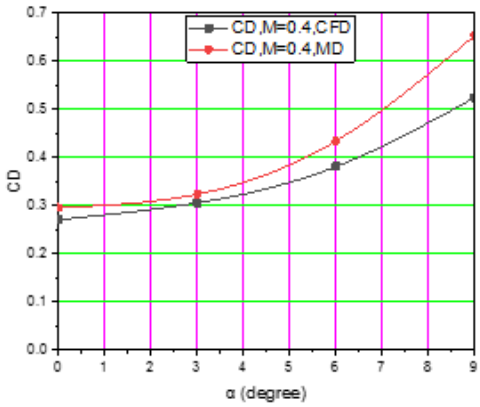

Figure 5. a: Total Drag force in the subsonic region

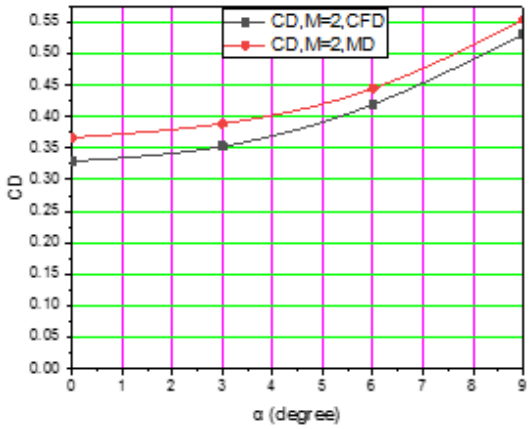

Figure 5. b: Total Drag force in the subsonic region

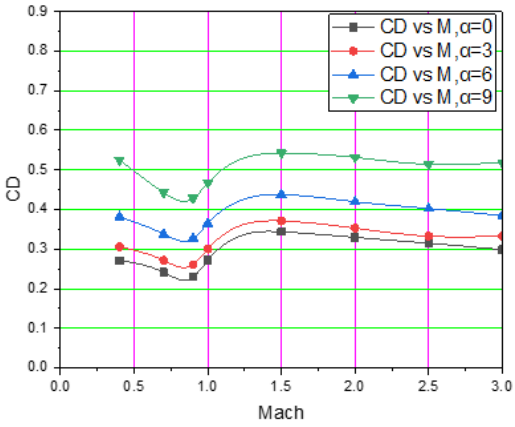

Figure 6: Total Drag coefficient versus velocity

Secondly, the missile DATCOM considered fins as a planner, but CFD uses the real shape of the fins and finally, the CFD considered boundary layer effect, but Missile DATCOM does not consider the boundary layer effect. Also, the effect of induced drag becomes dominated at a high angle of attack. The divergence between the two different calculation methods becomes small in the supersonic flow region this convergence refers to the shape of the shock wave being oblique in supersonic speed which has less strength compared with the normal shock wave, and shock wave detaches flow which reduces the effect of the boundary layer.

Figure 6 represents the total drag force coefficient for the whole region of speed and angle of attack. The total Drag coefficient increases with an increase in the angle of attack. The total Drag coefficient starts to decrease with the increase of speed because the friction drag has a strong effect on the body at low speed while this effect is reduced with an increase of speed.

With the continuous increase in speed till reaches the transonic regime and approximately at M = 0.9, the CD starts to increase sharply due to the effect of a normal shock wave which has the maximum wave drag. This increment in drag coefficient continuous until M = 1.6 and then with the increase of speed the Drag coefficient starts again to decrease slightly as shown in Figure 6. The decrease in total Drag at supersonic speed is a result of the shape of the shock wave which becomes oblique in supersonic speed with less strength compared with a normal shock wave that occurs at transonic speed.

Moreover, at supersonic regime, the oblique shock wave detaches the flow from the boundary layer which leads to reduction in skin friction drag and therefore reduction in the total drag coefficient at supersonic flow regime with the increase of Mach number. The Drag coefficient is very sensitive to the angle of attack since the highest values of drag are captured by the CFD and Missile DATCOM programs.

The effect of speed (Mach number) from subsonic to supersonic regions on the Drag coefficient is less compared with the airfoil profile that represents some dramatic phenomena. It is obvious in subsonic and supersonic regions, the Missile DATCOM program is representing high Drag coefficient than CFD results due to consideration of the wrap fins as planner fins in Missile DATCOM inputs.

Lift Force Coefficient

The lift coefficient is strongly affected by the fin parameters such as fins span, fins chord, thickness, leading-edge sweep, curvature radius, fin numbers, setting angles, and airfoil section. Figure 7 (a and b) illustrates the total lift force coefficient for various regions of speed.

Figure 7. shows the total lift force coefficient for the missile in the subsonic flow region at M=0.4 versus angle of attack. The lift coefficient predicted by the Missile DATCOM program increases gradually till the angle of attack is 3 °s where it is approximately 0.521 then increases sharply with high slop to 2.261 at a 9 °s angle of attack.

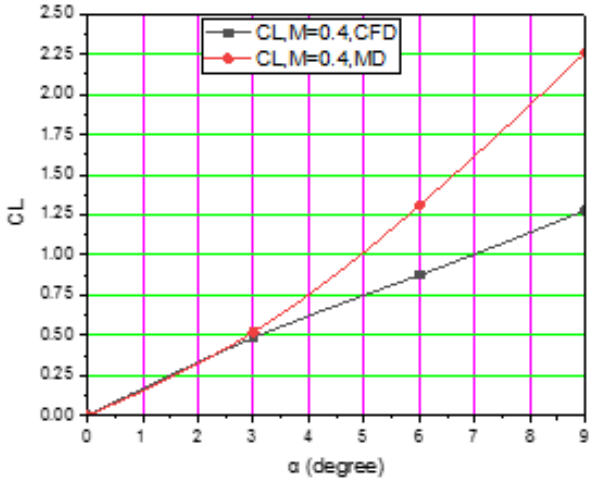

Figure 7. a: Lift force coefficient in the subsonic region

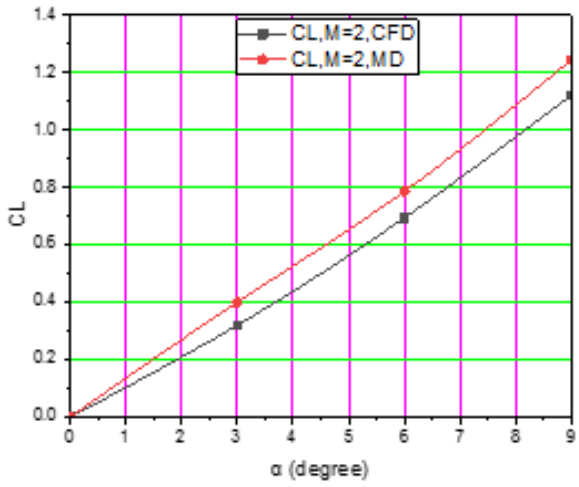

Figure 7. b: Lift force coefficient in the supersonic region

The lift coefficient that numerically calculated is reveals full agreement with the analytical result till 3 ° after that a large divergence is observed. The numerical program keeps the same slop till the 9 °s angle of attack where the lift coefficient is 1.2777. The difference in reading between the CFD method and Missile DATCOM method refers to fins shape. The CFD deals with real fins shape (wrap-around fins) whereas the Missile DATCOM deals with fins as planner fins.

Figure 8. b represents the total lift force coefficient for the missile in the supersonic flow region at Mach number 2 against the angle of attack. The figure provides an exact tendency between two programs with constant under-predicting of CFD till the angle of attack is 9 degrees.

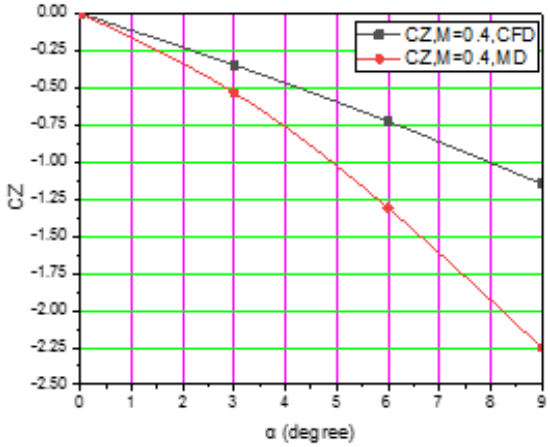

Figure 8. a: Total Side force in the subsonic region

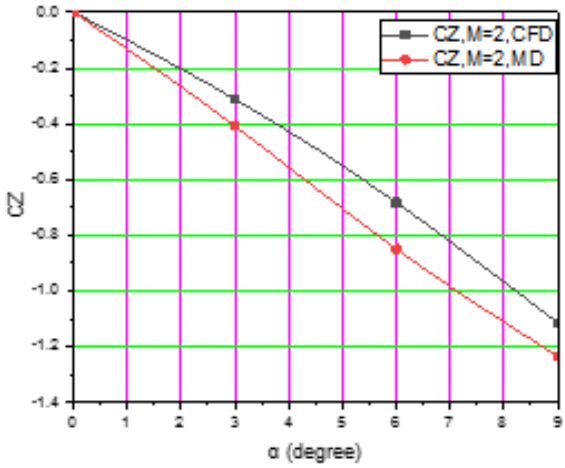

Figure 8. b: Total Side force in the supersonic region

The lift coefficient indicated by Missile DATCOM and computational technique at 9 degrees is 1.246 and 1.1219 respectively. No delay, but the constant divergence is captured between the two programs in supersonic regime up to 0.1241.

As stated before, the delay in under-predicting of numerical solution for the lift coefficient at a higher angle of attack results from the fact that the planner fins defined for the Missile DATCOM program generate more lift than the real wrap-around fins introduced to the numerical program, and the free stream was used in Missile DATCOM program.

Side Force Coefficient

It is well known that the single body is a critical symmetric geometry, which cannot generate the lateral force effectively. therefore, having wraparound fins (WAF), the entire rocket would have produced additional side force and side moment. Because of the effect of the angle of

attack, the pressure on the lower fins becomes higher than that of the upper fins.
These elements lead to an imbalance in the pressure distribution and generate the side forces which are normal to the plane of the free stream. Figure 8 (a and b): represents the total side force coefficient for various regions of speed.
Figure 8. a determines the total side force coefficient for the whole missile in the subsonic flow region at Mach number 0.4 versus angle of attack. Missile DATCOM program predicts -2.252 Side Force coefficient at 9 ° angle of attack whereas only -1.1467 is predicted by CFD at the same angle. The Missile DATCOM program represents a large change in Side Force coefficient along with the change of angle of attack compared with the Computational Fluid Dynamic in the subsonic region.
Figure 8. b illustrates the side force coefficient for the missile in the supersonic flow region at Mach number 2 versus angle of attack. The divergence between the codes is reduced to 0.1207 at 9 degrees angle of attack with an increase in the speed to supersonic speed.
The side force coefficient is -1.235 and -1.1143 at 9 degrees angle of attack predicted by MD and CFD respectively. The two methods have the same tendency and slop from approximately 3 ° angle of attack to 9 °. The over-predicting of CFD is reduced in supersonics speed.

Flow Visualization

It is well known that the single body is a critical symmetric geometry, which cannot generate the lateral force effectively. ANSYS (Fluent) software has a strong capability to visualize the results of the simulation in different aspects, the below section shows the flow field structure for some flow properties (such as static pressure, dynamic pressure, velocity, and density) through different regions of speed.
The colors at the left side of the figure indicate the value of flow property in each region of the flow field, the gradient in colors starts from red as a maximum value and decreases gradually till reaches blue as a minimum value of the property under study. Figure 9 shows the contours of flow properties in different speed flow regions in the case of the missile active phase.
Figure 9. a represents the flow field structure for static pressure in the subsonic flow region (M=0.7). It is evident from the figure that the highest value of static pressure is located at the nose of the missile due to the stagnation area concept. The pressure at this point reaches 3.71.104 Pa. Due to the ogive shape of the nose, the static pressure is changed along with the nose.
Starts from the nose tip and then decreases in value till the end of the nose. Thereafter, the value of the static pressure is constant until reaches close to the rear part of the missile. The static pressure starts increasing as a result of the sudden decrease in the diameter of the rocket. The figure shows that the lowest value for static pressure is -1.66.104 Pa in the blast area because it is a very high-speed zone.
Figure 9. b shows the contour of the static pressure in the sonic flow region.
It can be seen that the value of the static pressure at the transition speed is starting to change its value 8.64.104 Pa at the head of the nose, where the highest value of the static pressure to -2.2.104 Pa at the end of the nose of the missile where the pressure is very low due to the presence of shock waves in the flow.
This region represents the area of expansion because the shock wave always is accompanied by an expansion wave where the speed increases and the pressure decrease (Bernoulli principle). It is also noticed that there is another shock wave presented in the tail area with less strength than the forward wave due to the deceleration of flow passing to the tail orientation.
Figure 9. c reveals the flow field structure for static pressure in the supersonic flow region where M=2. According to the figure in the supersonic zone, the shock wave is still presented, but it becomes more oblique and closer to the missile body, with a small wave drag compared to the normal shock wave.

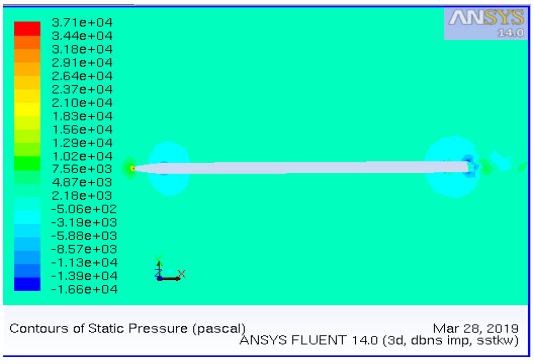

Figure 9. a: Static Pressure in subsonic region

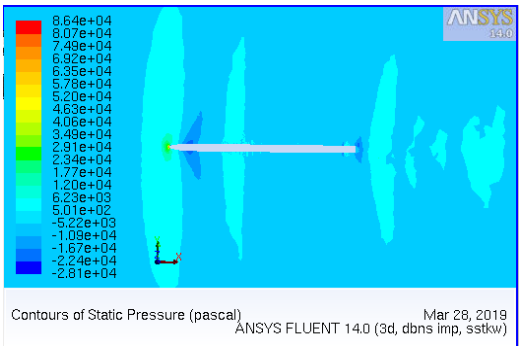

Figure 9.b: Static Pressure in sonic region

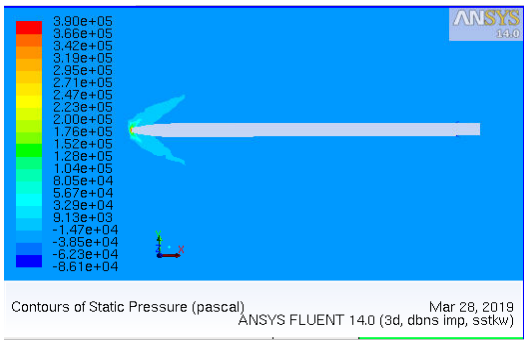

Figure 9. c: Static Pressure in the supersonic region

Figure 10 represents the contour of dynamic pressure for different flow regions. Figure 10. illustrates the flow field structure for the dynamic pressure in the subsonic flow region (M=0.7). It is observed from the figure that the highest value of the dynamic pressure is 3.71.104 Pa located at the area of the missile's nozzle, where the less value is 3.71.102 Pa at the tip of the missile because of stagnation flow position.

Moreover, the flow contact with the missile's body has a very low dynamic pressure because the speed on the surface is very slow as a result of friction and boundary layer generation impact. Figure 10. b shows the contour of the dynamic pressure in the transonic flow region. The highest value of dynamic pressure is 3.89.105 Pa located at the missile's nozzle area.

At the speed of sound, the shock wave is captured at the front part of the missile. As a result of the shock wave appearing, the dynamic pressure reaches a very high magnitude of 2.92.105 Pa at the shock wave area. At the rest of the missile's body, the flow experiences a low dynamic pressure of 1.56.105 Pa as a result of the no-slip condition and boundary layer exhibition. Figure 10. c represents the contour of dynamic pressure in the supersonic flow region with Mach number 2.

The Figure reflects the highest value of dynamic pressure which is 9.48.105 Pa located at the area of the missile's nose. It is justified that the shock wave at the tip of the warhead is more oblique towards the body of the missile.

This oblique shock has less strength than the vertical shock wave. The high velocity encourages the flow to separate, which leads to an increment in boundary layer thickness. This part of the flow contact to the missile body has a very low value of dynamic pressure 4.74.105 Pa.

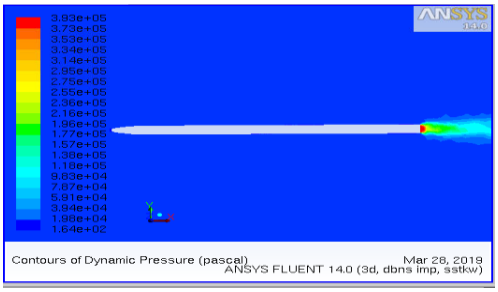

Figure 10.a: Dynamic Pressure in the subsonic region

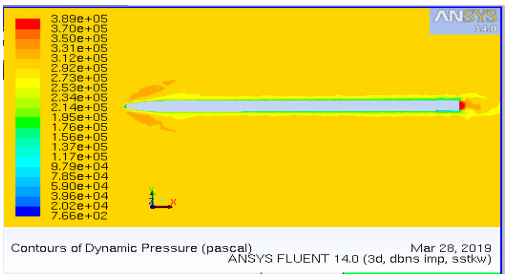

Figure 10. b: Dynamic Pressure in sonic region

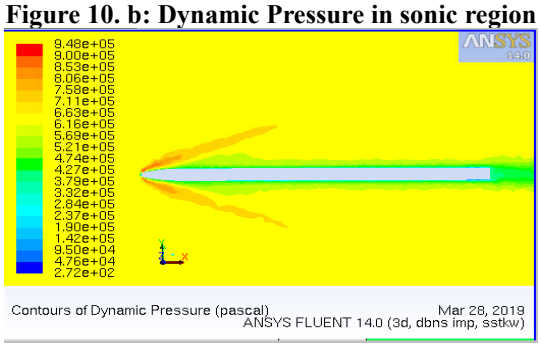

Figure 9. c: Dynamic Pressure in the supersonic region

CONCLUSIONS

Flow field solutions of GRAD rocket were obtained using the computational fluid dynamics techniques that utilize the ANSYS/FLUENT program as a simulation program. Mesh was accurately generated and validated across the flow field, both near the tip of the rocket nose and at the fin edge of

the rocket. Simulations have been performed at Mach numbers from 0.4 to 2 for maximum allowable 9° angle-of-attack and sideslip angle range from 0 degrees to 9 degrees. °.

The total drag of the whole rocket is mainly generated from the body, while the drag produced by the wrap-around fins is about 18.45 percent. The total drag coefficient increases proportionally with the angle of attack while its inverse is proportional to the Mach number in the subsonic region. Maximum total drag presence at 1.6 Mach number at all range of angle of attack.

With the increase of speed in the supersonic region, the Drag coefficient starts again to decrease slightly, but not less than the subsonic regime. The decrease in total drag at supersonic speed is a result of an oblique shock wave in supersonic speed. The Missile DATCOM software was used to verify and validate the CFD's results which represent a satisfactory agreement between them.

REFERENCES

[1] http://charaterisationexplosiveweapons.org/studies/annex-a-122-mm-mbrl/

[2] Slobodan Mandic, (2006), "Analysis of the Rolling Moment Coefficients of a Rocket with Wraparound Fins", *Scientific-Technical Review, Vol. LVI, No.2, 2006,* UDK: 533.665:533.694.52, COSATI: 16-04, 20-04, 01-01

[3] Ravi Krishna, Rhishabh Surit and Ajoy Ghosh, *(2009),* "Anomalies in the Flow over Projectile with Wraparound Fins", *Defence Science Journal, Vol. 59, No. 5, pp. 471-484 Ó2009, DESIDOC*

[4] *Attapon Charoenpon, Ekkarach Pankeaw, (2011), "*Method of Finding Aerodynamic Characteristic Equations of Missile for Trajectory Simulation*", International Journal of Aerospace and Mechanical Engineering Vol:5, No:9*

[5] F. Mingireanu, L. Georgescu, G. Murariu and I. Mocanu, *(2014),*"Trajectory Modeling of GRAD Rocket with Low-cost Terminal Guidance Upgrade Coupled to Range Increase Through Step-like Thrust-curves", *Rom. Journ. Phys., Vol. 59, Nos. 3–4, P. 369–381, Bucharest*

[6] *Chun-Chi Li, Chang-Sheng Tai, Cheng-Chyuan Lai, Shang-Min Fu and Yen-Chun Tsai, (2013),"*Study of the Aerodynamic Characteristic and Flight Trajectories in a Tail Fin-Stabilized Projectile with Different Shapes*", 37th National Conference on Theoretical and Applied Mechanics*

[7] Guo Qing Zhang, S. C. M. Yu and Jorg Schluter, *(2016)*,"Aerodynamic Characteristics of a Wrap-Around Fin Rocket", *Aircraft Engineering and Aerospace Technology: An International Journal, Vol, 88, No. 1, pp. 82–96*

[8] Anderson J D, (1991), "Fundamentals of Aerodynamics", *Book published by Mc Graw Hill publication. ISBN 0-07-001679-8*

*[9] Wilcox, D. C., (2008), "*Formulation of the k-omega Turbulence Model Revisited*", AIAA Journal, Volume 46, Number 11, pp. 2823-2838.*